# P1.1 AIR-SEA INTERACTION PROCESSES IN WARM AND COLD SECTORS OF EXTRATROPICAL CYCLONIC STORMS OBSERVED DURING FASTEX

P. Ola G. Persson[1], J. E. Hare[1], C. W. Fairall[2], and W. Otto[2]
[1]CIRES/NOAA/ETL, Boulder, CO
[2]NOAA/ETL, Boulder, CO

## 1.OBJECTIVES

- Study the modulation of air-sea interaction processes by mid-oceanic storms
- Study how these processes in turn impact the structures important for the development of these storm systems, especially the dynamically important warm sector region
- Validate satellite-based measurements of basic near-surface atmospheric parameters in specific regions of the storms

## 2. METHOD

### 2.1 Available Data

Fronts and Atlantic Storm Tracks Experiment (FASTEX) field program (Dec. 1996-Feb. 1997)

Mid-Atlantic ships (30-40 W, 40-50 N)
- *R/V Knorr*, *R/V Suroit*, *Victor Bugaev*, *Aegir*
- basic meteorological parameters
- 1.5-6 h soundings

On *R/V Knorr*
- surface fluxes of momentum (t), sensible heat ($H_s$), and latent heat ($H_l$) through covariance, inertial dissipation, and bulk methods (Fig. 1a)
- wave height spectrum from TSK recorder (Fig. 1b)
- subjective manual estimates of sea-surface conditions, including swell and wave directions by ships crew on the bridge

### 2.2 Data compositing

**Composite the observations in a storm-relative framework**

Method and definitions (example in Fig.2)
- Near-surface specific humidity a key parameter to define the onset of the warm-sector region and the end of the post-frontal region
- Warm sector region: period between the increase in the surface specific humidity and the wind shift
- Surface cold frontal passage: time of surface wind direction shift
- Post-frontal regime: period between the wind shift and the end of the decrease in specific humidity

Typical changes in air temperature, wind speed, surface pressure, and precipitation often seen though not used to define the transitions

**SUMMARY OF COMPOSITING EFFECT (Table 1)**

- 10 cases for the *R/V Knorr*.
- warm sector duration averaged 17.5 hours, ranging from 3.1-43.4 hours.
- post-frontal regime duration averaged 8.4 hours
- cases 1-7 obtained south and east of the Gulf Stream sea-surface temperature front (average SST=16.1 C)
- cases 8-10 obtained in the colder waters to the north and west of this front (average SST=3.5 C).
- storms' movements past each ship produced a northeast-to-southwest time-to-space adjusted "track" for each ship through each storm (Fig. 3). The orientation and path of the storm determined the obliqueness of the ships' tracks relative to the frontal cloud bands. For example, the tracks were nearly orthogonal to the surface cold front in cases 3 and 6, while they were nearly parallel for cases 4 and 8.

**USE OF COMPOSITING METHOD**

Statistical composites of storm-relative atmospheric parameters, wave characteristics, and surface fluxes were computed for each ship. The composites were temporally normalized using the duration of the warm sector region for each case. Hence the warm sector occurs for a normalized time of -1 to 0 and the post-frontal region for a normalized time of 0 to 1. The difference in duration between the post-frontal region and the warm sector led to few samples during the latter half of the normalized post-frontal region. Only the composited data from the *R/V Knorr* are presented here.

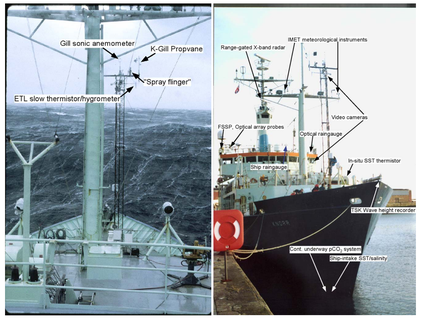


*Fig. 1: Placement of instrumentation on board the R/V Knorr as viewed from a) the bridge towards the bow during a storm and b) in front of the ship.*

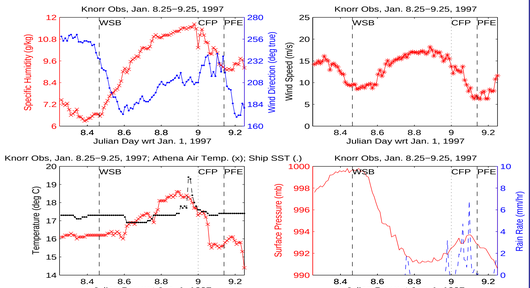


*Fig. 2: Time series of a) specific humidity (x) and wind direction (dot), b) 18-m wind speed, c) sea surface (dot) and air (x) temperatures, and d) surface pressure (solid) and rain rate (dashed) from the R/V Knorr for case 4 (JD8.25-9.25). The onset of the warm sector (WSB), the cold-frontal passage (CFP), and the end of the post-frontal regime (PFE) are marked by dashed and dotted lines.*

*Table 1: Characteristics of the 10 FASTEX cases used for compositing the R/V Knorr data.*

| Case | Warm sector duration (hr) | Cold-frontal passage (decimal Julian day) | Post-frontal sector duration (hr) | System phase velocity (m s$^{-1}$/ deg) | 15-min, 18 m LLJ wind speed max (m s$^{-1}$) | Avg. SST (deg C) |
|---|---|---|---|---|---|---|
| 1 | 16.44 | 4.885 | 3.48 | 18.4/210 | 21.5 | 15.0 |
| 2 | 3.12 | 5.190 | 15.84 | 11.6/225 | 19.1 | 15.4 |
| 3 | 18.62 | 7.776 | 6.58 | 18.7/254 | 19.6 | 17.4 |
| 4 | 12.84 | 9.0 | 3.36 | 33.4/240 | 19.0 | 17.4 |
| 5 | 3.50 | 9.425 | 2.76 | 26.4/233 | 21.3 | 17.3 |
| 6 | 7.92 | 12.99 | 4.80 | 25.0/258 | 18.6 | 15.4 |
| 7 | 43.44 | 20.21 | 16.08 | 23.2/229 | 20.0 | 14.5 |
| 8 | 15.36 | 22.05 | 13.20 | 27.4/234 | 18.3 | 3.4 |
| 9 | 28.32 | 24.08 | 12.48 | 25.7/266 | 18.0 | 4.0 |
| 10 | 25.68 | 26.37 | 5.52 | 27.3/234 | 22.0 | 3.2 |
| Average | 17.5 | N/A | 8.4 | 23.7/238 | 19.7 | 16.1/3.5* |

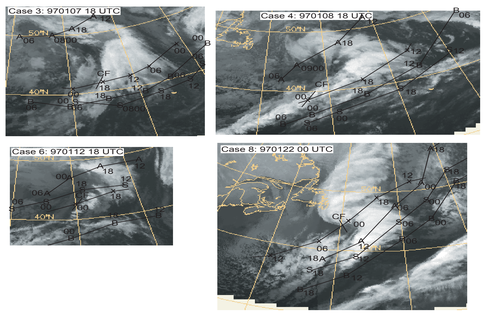


*Fig. 3: Time-to-space converted tracks of the research vessels* Knorr *(x),* Aegir *(A),* Victor Bugaev *(B), and* Suroit *(S) through cases 3, 4, 6 and 8. The overlaid infrared satellite image corresponds to a time shortly prior to when the* R/V Knorr *passed through the surface cold front. The times next to each symbol marks the hour at that location.*

## 3. SURFACE LAYER DESCRIPTIONS

### Atmospheric

**Atmospheric parameters show regular variations relative to cold-frontal passage**

- air temperature shows an increase of about 4°C from the onset of the warm sector to just before the cold frontal passage, dropping behind the cold front (Fig. 4a)

- specific humidity increases nearly 4 g kg$^{-1}$ within the warm sector, peaking just before the cold-frontal passage (Fig. 4b)

- wind speed shows the surface-layer manifestation of the classical low-level jet shortly before frontal passage, with an increase of about 8.5 m s$^{-1}$ from the onset of the warm sector (Fig. 4c). The maximum composite wind speed was about 17 m s$^{-1}$ in the warm sector, though the maximum 15-min 20-m wind speeds during the warm sector averaged 19.7 m s$^{-1}$, and ranged from 18-22 m s$^{-1}$ (Table 1). The wind speed initially drops at the cold frontal passage, but then increases to another peak in the post-frontal region. Note that the onset of the wind speed increase occurs west of the eastern edge of the warm sector, as defined by the specific humidity. Hence, the thermodynamic and kinematic definitions of the warm sector region aren't exactly coincident.

- in the transition from the eastern edge of the warm sector, the wind direction initially has a more westerly component than at the cold frontal passage, and then a slightly more easterly component (Fig. 4d). This implies that the surface-layer flow is diffluent at the eastern edge of the warm sector, and then becomes slightly confluent near the middle of the warm sector.

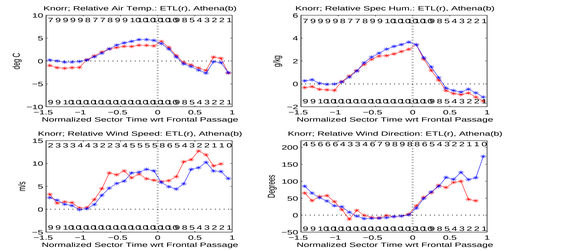


*Fig. 4: Composite relative values of a) temperature, b) specific humidity, c) wind speed, and d) wind direction with respect to the cold frontal passage from the R/V Knorr. Values are relative to their values at the onset of the warm sector, except for wind direction, which is relative to the value 1 hour before frontal passage. The red line shows the data from the ETL sensors and the blue line those from the ship's Athena data system. The numbers along the top and bottom of each frame shows the number of cases that contributed to each composite bin for the ETL sensors (top) and Athena sensors (bottom).*

### Oceanic

**Wave characteristics show regular and physical variations relative to cold-frontal passage**

-significant wave heights (the mean of the highest one-third wave heights) increased from about 2.3 m in the eastern half of the warm sector to about 3.9 m at the time of frontal passage (Fig. 5a). The maximum wave heights were about 5.5 m in the eastern half of the warm sector increasing to about 9 m at the time of frontal passage.

- period of the significant waves was at a minimum of 6.5 s within the eastern half of the warm sector,and reached a maximum of 7.8 - 8.0 s shortly after frontal passage (Fig. 5b). Hence, wave growth and an increase of the wave period occurs within the warm sector to just after the cold frontal passage. Note that the changes in wave height and period doesn't occur until after the onset of the increase in the wind speed, which occurs after the ship has been in the warm sector for 2-3 hours.

-since high-frequency (low period) waves tend to respond more quickly to changes in the wind than low-frequency (large period) waves, splitting the wave data into wave period bins is useful. We find the following:

1) the frequency of occurrence of waves with periods > 6 s increases in the last two-thirds of the warm sector at the expense of the waves with periods < 6 s (Fig. 5c), and

2) the mean height of the waves with periods >3 s increase in the warm sector (Fig. 5d). The response in the wave height occurs first for the short period waves.

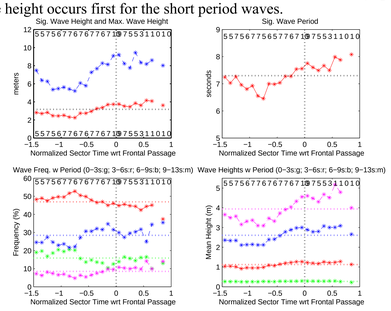


*Fig. 5: Composite values of a) significant (red) and maximum (blue) wave heights, b) significant wave period, c) wave frequency for different wave period bins , and d) wave height for different wave period bins with respect to the cold-frontal passage from the R/V Knorr. The wave period bins in c) and d) are 0-3 s (green), 3-6 s, (red), 6-9 s (blue), and 9-12 s (magenta).*

## 4. SURFACE FLUXES

**Variations of τ, $H_s$ and $H_l$ relative to location of surface front**

-Covariance stress (t) increase begins at a normalized time of -0.75 (Fig. 6a), which is the time the wind speed increases (Fig. 4c) and the wave characteristics respond (Fig. 5). The peak t of 0.7 N m$^{-2}$ occurs a little before the cold frontal passage at the time of maximum wind speed, peak in the occurrence of the 6-9 s period waves, and near the peak in heights of these waves. Comparably high values of t also occur in the post-frontal regime, roughly corresponding to the time of the secondary wind speed maximum.

-Sensible heat flux ($H_s$) is a maximum in the post-frontal regime and before the onset of the warm sector (Fig. 6b). Within the warm sector, $H_s$ decreases as the front approaches the ship, becoming slightly negative just before the passage of the surface cold front. Qualitatively, this is consistent with the warming of the prefrontal air through horizontal advection and surface-layer fluxes producing a stable environment nearest the front and hence negative $H_s$ (e.g., Bond and Fleagle, 1988).

-Latent heat flux ($H_l$) also decreases within the warm sector (Fig. 6c) as the specific humidity increases (Fig. 4b). However, in contrast to $H_s$, $H_l$ remains positive. The maximum $H_l$ occurs just before the onset of the warm sector and at the very end of the post-frontal regime.

**Variations of stress direction relative to location of surface front and to swell direction**

The covariance stress components can be used to compute a stress direction. If the stress is due entirely to wind waves, then the stress direction should be the same as the wind direction. If the swell is influencing the stress, then the stress direction should be between the swell and wind directions. The composite of the difference between the stress and wind directions show that in the western portion of the warm sector, the stress direction is usually greater than the wind direction by 5-12° (that is, the stress direction is to the right of the wind direction), while in the post-frontal regime the opposite appears to be true (Fig. 6d). Cross-stream stress errors due to anemometer tilt errors should be fairly small since the stability is near neutral in these high wind conditions (Wilczak et al 2001). Manual observations of the swell direction show that the stress direction is frequently between the swell direction and the wind direction. For the example in Fig. 7, a difference between the wind direction and swell direction occurs only in the two warm sectors. Hence, the difference between the wind direction and stress direction occurs only in the warm sector for these two cases. Other cases produce the post-frontal regime differences shown in Fig. 6d. These results suggest that in the vicinity of fronts, the stress vector may not be an accurate indicator of the wind direction. This has significant implications for remote sensing of surface winds over the oceans, and the use of such winds in diagnosing storm dynamics.

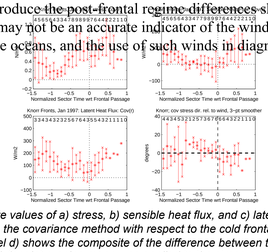


*Fig. 6: Composite values of a) stress, b) sensible heat flux, and c) latent heat flux determined from the covariance method with respect to the cold frontal passage from the R/V Knorr. Panel d) shows the composite of the difference between the stress direction and wind direction. A 3-point running mean was applied to the stress components before the stress direction was calculated. The vertical errors bars show ± one standard deviation.*

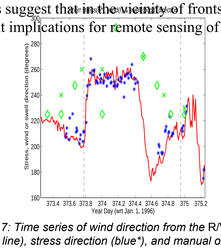


*Fig. 7: Time series of wind direction from the* R/V Knorr *(red line), stress direction (blue*), and manual observations of the swell direction from two different ship logs (green diamond, green "x") for the period Julian Day 373.3 – 375.25. The two vertical dashed lines show the frontal passages for cases 1 and 4.*

**Differences in front-relative variations between covariance, inertial dissipation (ID) stress and $H_l$ fluxes**

Surface fluxes from ID calculations (Figs. 8a-c) and the bulk flux relationships of Fairall et al (2003) (Figs. 9a-c) show the same qualitative trends that was noted for the covariance fluxes (Fig. 6). However, the ID stresses are slightly smaller than the covariance stresses, especially in the higher wind speed regime in the vicinity of the fronts. Furthermore, the ID sensible heat fluxes are lower near the fronts and higher in other areas. The differences in $H_l$ are not as systematic, though there is still a tendency for the ID $H_l$ to be weaker in the vicinity of the front. The bulk flux differences plot (Fig. 9d) shows that the bulk stresses are substantially (up to 0.25 Nm$^{-2}$) smaller than the covariance ones, particularly in the post-frontal regime, and that the bulk $H_s$ are 10-20 Wm$^{-2}$ less than the covariance ones, especially in the vicinity of the fronts. The bulk $H_l$ appear to be larger in the warm sector and smaller in the post-frontal regime. The reasons for the differences between the covariance, ID, and the bulk fluxes are currently under investigation. These reasons may include flow distortion or ship-motion problems, real differences due to the assumptions inherent in the ID (e.g., see Appendix in Fairall et al 2003) and bulk techniques, and the effects of the wave conditions in the vicinity of the fronts.

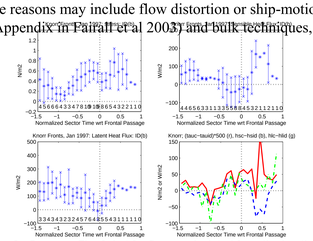


*Fig. 8: Same as Fig. 6, but for fluxes calculated from the inertial dissipation technique. Panel d) shows the differences in the fluxes between the covariance and the inertial dissipation techniques. Note that the stress differences have been multiplied by 500 to scale properly on the plot.*

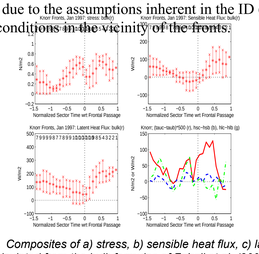


*Fig. 9: Composites of a) stress, b) sensible heat flux, c) latent heat flux calculated from the bulk formulas of Fairall et al. (2002). In d), the differences between the covariance and bulk values of stress (red), Hs (blue) and Hl (green) are shown. Note that the stress differences have been multiplied by 500 to scale properly on the plot.*

## 5. CONCLUSIONS

**Composites of atmospheric surface layer measurements show that:**

**a)** The momentum flux is a maximum just before the frontal passage during the peak in wind speed associated with the warm-sector low-level jet. A second stress maximum of comparable magnitude occurs in the middle of the post-frontal regime for the data from the *R/V Knorr*. The *R/V Suroit* data cases (not shown in this study) does not show the post-frontal maximum.

**b)** The latent and sensible heat fluxes are a minimum just before the frontal passage. Despite the strong surface winds at this time, the moistening and warming associated with synoptic-scale advective patterns and surface-layer fluxes minimize the vertical gradients in specific humidity and temperature. This pattern should affect the surface potential vorticity generation, and has dynamical implications for the stability of the cold-frontal zone for frontal wave development.

**c)** Wave heights increase steadily from the eastern half of the warm sector until frontal passage, remaining high through most of the post-frontal regime before decreasing.

**d)** Differences between covariance and inertial dissipation fluxes are largest during the times bracketing the cold front when the wave heights of the waves with period 6-9 seconds are large and the covariance fluxes are large.

**e)** The stress direction is consistently 5-12° to the right of the wind direction in the warm sector and 2-15° degrees to the left of the wind direction in the post-frontal regime. This implies that satellite-based scatterometer wind directions, which rely on the surface stress field, will underestimate the surface directional wind shift across the front.